doi:10.3788/gzxb20164507.0706005

一种高质量最小波长的超低损耗锥形光纤设计

李建辉[1],张永棠[1],王访[2]
(1 广东东软学院 计算机科学与技术系,广东 佛山 528225)
(2 湖南农业大学 管理学院,长沙 410000)

摘 要:采用火焰刷法对单模光纤进行加热拉锥,形成具有微纳米量级纤芯半径的光波导结构,并引入不同的绝热系数对低损耗锥形光纤进行优化,使其满足绝热标准.设计出恒定锥角为 2 mrad、波长为 400 μm、纤维半径为 4 μm 具有最佳形状的低损耗锥形光纤.Matlab 仿真结果表明,23 mm 长的低损耗锥形光纤传输透视率为 99.7%,63 mm 长的低损耗锥形光纤抗辐射能力达到 99.6%.由于功率被耦合到高阶模式,其损失被充分抑制,具有恒定锥角的锥形光纤可以实现不牺牲传输质量的光耦合传输.

关键词:光通信;最小波长;锥形光纤;实验研究;传输质量
中图分类号:TN253; TN914 **文献标识码**:A **文章编号**:1004-4213(2016)07-0706005-6

The Design of a High Quality and Minimum Wavelength of Ultra-low-loss Tapered Optical Fiber

LI Jian-hui[1], ZHANG Yong-tang[1], WANG Fang[2]
(1 *Department of Computer Science and Technology, Guangdong Neusoft Institute, Fushan, Guangdong* 528225, *China*)
(2 *School of Management, Hunan Agricultural University, Changsha* 410000, *China*)

Abstract: The single-mode fiber was heated tapering by flame brush method, forming an optical waveguide structure which has a core radius of micro-nanometer level, and the low-loss optical fiber tapered was optimized by the different coefficients of thermal insulation to meet insulation standards. The tapered optical fiber with the best shape was designed, whose constant cone angle is 2 mrad, wavelength is 400 μm and fiber radius is 4 μm. Matlab simulation results show that, the transmission perspective of tapered optical fiber with length of 23 mm is 99.7%, the radiation resistance of tapered optical fiber with length of 63mm is 99.6%. Since the power is coupled to the high-order mode, the loss is sufficiently suppressed, so that the optical coupling transmission of the tapered fiber with a constant taper angle can be achieved without sacrificing the quality of the transmission.

Key words: Optical communication; Minimum wavelength; Tapered Optical Fiber(TOF); Experimental research; Transmission quality
OCIS Codes: 060.2280; 060.2340; 060.4005; 060.4264

0 Introduction

The tapered optical fibers with a sub-wavelength waist radius have been utilized for diverse applications in photonics and quantum optics[1-2]. Strong confinement of the guided mode to a sub-wavelength radius leads to efficient nonlinear effects such as super continuum generation[3] and third-harmonic generation[4]. Large evanescent fields of the guided mode are beneficial for optical sensing and

Foundation item: The National Natural Science Foundation of China (No. 31501227), Jiangxi province science and technology innovation project (No. GJJ12255)
First author: LI Jian-hui(1974—), male, associate professor, Ph. D. degree mainly focuses on optical communication and sensing network. Email:joe863@163.com
Corresponding author: ZHANG Yong-tang(1981—), male, associate professor, M. S. degree, mainly focuses on optical communication and sensing network. Email:1141760796@qq.com
Received: Nov. 30, 2015; **Accepted**: Apr. 6, 2016

spectroscopy[5]. realizing strong light-matter interaction[6-7]. And coupling to whispering-gallery-mode micro resonators[8-9]. For these applications, minimizing Tapered Optical Fiber (TOF) losses is important and sometimes crucial. In addition to extrinsic losses caused by surface roughness or contaminants, there are more fundamental TOF losses caused by the power coupling from the fundamental mode to higher-order modes because of the non-zero taper angles[10-11]. These power coupling losses depend on the TOF shape; TOFs with smaller taper angles, *i.e.*, more adiabatic shapes, have lower power coupling losses. Transmissions of 99.4% and 99.95% have been achieved using TOFs with an exponential shape with a decay constant of 10mm[12] and using TOFs with a constant taper angle of 2 mrad[13-14], respectively. However, TOF with small taper angles tend to be long (the lengths of the exponential TOF in Ref. [25] and the 2 mrad TOF in Ref. [22] are 111 mm and 84 mm, respectively); there is a trade-off between the short length and high transmission of TOFs.

For some applications, *e.g.*, fiber coupling to micro resonators, shorter TOFs is desirable because of their higher mechanical stability. Moreover, there is sometimes a constraint on the length of the TOFs when they are installed in small spaces, such as cryostats[15] or vacuum chambers[16]. Therefore, it is desirable to restrict the length of the TOFs as much as possible while maintaining high transmission. Useful guidelines for designing such TOFs are the adiabaticity criteria[17], which give the upper limit for the local taper angle as a function of the local taper radius. There have been studies reporting the fabrication of TOFs containing three tapered sections where each section has a different taper angle so that the taper angle is smaller where the adiabaticity criterion gives a smaller upper limit[18-19]. Although transmissions higher than 99% have not been achieved with such trilinear TOFs, they can in principle have shorter TOF lengths than linear TOFs without sacrificing the transmission quailties. However, there have been no reports on the design and fabrication of TOFs with the shapes optimized in systematic ways for achieving minimal TOF lengths.

In this paper, we design and fabricate TOFs that optimally satisfy the adiabaticity criterion. We adopt the flame-brush method[20] using variable torch scan lengths, and we optimize the scan length so that the local taper angle satisfies the adiabaticity criterion by taking a systematic approach. We accordingly fabricate TOFs with optimal shapes and compare their transmission with those having a constant taper angle of 2 mrad and those having an exponential shape with a decay constant of 3 mm. To investigate the reproducibility, five samples are fabricated for each profile.

1 Theoretical researches

1.1 Adiabaticity criteria

A TOF is adiabatic if the taper angle is small enough so that there is negligible power coupling from the fundamental mode to higher-order modes. Adiabaticity criteria have been proposed to delineate such conditions[21]. The delineation angle $\Omega(r)$ as a function of the local taper radius r is given by the following length-scale criterion[19,21]

$$\Omega(r)=\frac{r}{2\pi}[\beta_1(r)-\beta_2(r)] \tag{1}$$

where $\beta_1(r)$ and $\beta_2(r)$ are the propagation constants of the fundamental (HE_{11}) and the first excited (HE_{12}) modes, respectively. If the local taper angle $\theta(r)$ is much smaller than $\Omega(r)$, the mode coupling is negligible and the fundamental mode propagates adiabatically. We introduce an adiabaticity factor F (>0) to express this condition as

$$\theta(r)<F\Omega(r) \tag{2}$$

Smaller F values lead to reduced mode coupling. Fig. 1 shows the delineation angle of a step-index fiber calculated with Mathematical (Wolfram Research) using the three-layer model[22] with the wavelength $\lambda=852$ nm and with the refractive indices and the radiuses of the core (cladding) of $n_{core}=1.457\,4$ ($n_{clad}=1.452\,5$) and $r_{core}=2.4$ μm ($r_{clad}=62.5$ μm), respectively.

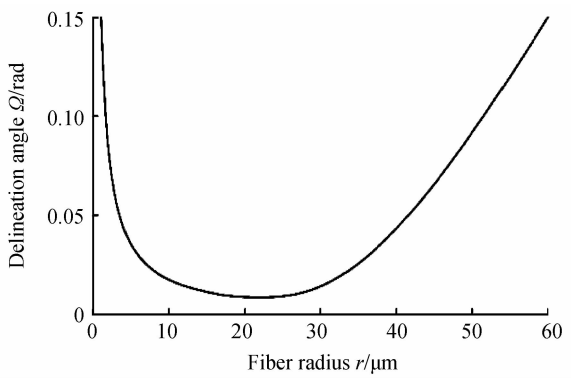

Fig. 1 Delineation angle and radius of the fiber

1.2 Model for the TOF shape

We model the shape of a TOF fabricated using the flame-brush method[23] with a variable torch scan length. In this method, a small flame heats a small region of a fiber with an initial radius r_0 to the softening point. While the fiber is pulled from both ends with a constant velocity v_1, the flame scans back and forth along the fiber axis with a constant velocity v_2. The length of the k-th scan is L_k. Here we count k by the number of one-way scans, not by the number of roundtrip scans. This scanning process elongates the

heated region of the fiber, and its radius is reduced to r_k after the k-th scan of the torch.

Fig. 2 shows the schematic of the TOF after the k-th scan. The origin of the z-axis is taken as the position of the torch at the beginning of the k-th scan (i.e., at the end of the $(k-1)$-th scan). The torch scans in the positive direction over a length of L_k, and the radius is reduced from r_{k-1} to r_k after the k-th scan. We assume that the flame width is small enough that a negligibly short length of the fiber is heated at any given time. As shown in Fig. 2, the cylinder with radius r_{k-1} and length ooo between planes labeled A and B is heated during the k-th scan and become a cylinder with radius r_k and length ppp between planes labeled A′ and B′ at the end of the k-th scan. The conservation of the volume before and after the k-th scan expressed as

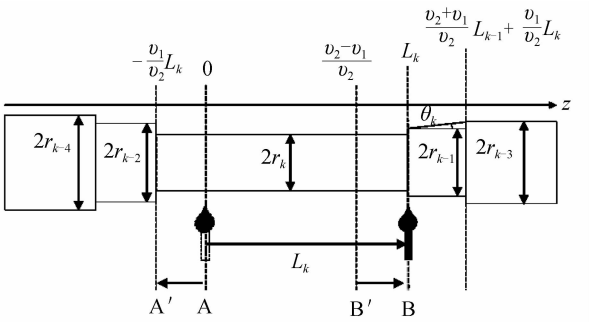

Fig. 2 The schematic of the TOF after the k-th scan

$$\pi r_k^2\left(\frac{v_2+v_1}{v_2}\right)L_k=\pi r_{k-1}^2\left(\frac{v_2-v_1}{v_2}\right)L_k \tag{3}$$

Leads to the a recurrence relation for the fiber radii as

$$r_k=\sqrt{\frac{v_2-v_1}{v_2+v_1}}\,r_{k-1} \tag{4}$$

The local taper angleθ_k after the k-th scan can be derived from Fig. 2 as

$$\tan\theta_k=\frac{r_{k-3}-r_{k-1}}{\left(\frac{v_2+v_1}{v_2}L_{k-1}\right)-L_k} \tag{5}$$

Note that this model is invalid if the torch passes the end of the heated region for the $(k-2)$-th scan,

$$L_k>\frac{v_2+v_1}{v_2}L_{k-1}+\frac{v_1}{v_2}L_k \tag{6}$$

This requirement poses the limitation as

$$L_k<\left(\frac{v_2+v_1}{v_2-v_1}\right)L_{k-1} \tag{7}$$

The total TOF length L_{total} after the n-th scan can be written as

$$L_{\text{total}}=\left(\frac{v_2+v_1}{v_2}\right)L_1+\sum_{k=2}^{n}\frac{2v_1}{v_2}L_k \tag{8}$$

1.3 Optimization of the heat length profile

To design an adiabatic TOF with minimal length, L_{total} must be minimized under the condition$\theta_k<F\Omega(r=r_k)$ for any k. For given values of r_0 and v_1/v_2, this minimization is an optimization of $L_k(k=1,2,\cdots,n)$. Note that a smaller value of the ratio v_1/v_2 leads to smaller staircase-step changes in the fiber radius (see Eq. (5)), thus leading to a smoother taper at the cost of larger number of total scans n. In our typical experimental conditions, there are approximately 300 total scans, $n\sim300$, which has too many degrees of freedom for a straightforward optimization. To reduce the degrees of freedom, we assume that L_k is a smooth function of k, which should be a reasonable assumption, considering the smooth shape of $\Omega(r)$ (see Fig. 1). Specifically, we consider a Lagrange interpolating polynomial, which passes through nine points that are fixed with even intervals on the scan-number axis k and are variable on the L axis, as L_k.

In addition to the conditions given by Eqs (3) and (7), we pose the following conditions. First, we introduce the upper limit for L_k of $L_{\text{upper}}=40000\,\mu$m to take into account of the limitations of the experimental setup. Second, we introduce the lower limit for L_k of $L_{\text{lower}}=400\ \mu$m to take into account of the finite width of the flame. Furthermore, because the delineation angle $\Omega(r)$ abruptly increases as r becomes less than $\sim4\ \mu$m, we fix L_k as $L_k=L_{\text{lower}}$ for $r_k\leqslant4\ \mu$m. This restriction gives better results than optimizing L_k for the whole indices of k.

We optimize L_k with the downhill simplex method[24], starting from ten sets of random initial values. The numerical calculation is performed with custom scripts using Matlab (Math-Works). Fig. 3 shows the optimized profiles of L_k with the adiabaticity factors of $F=0.2$, 0.4, 0.6, and 0.8. The TOF with larger F values require longer scan lengths, which leads to longer TOF lengths.

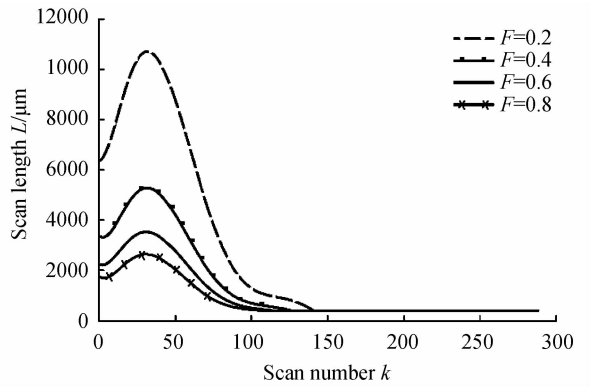

Fig. 3 Optimization of insulation factors and TOF take longer to scan length diagram

2 Experimental researches

We experimentally fabricate TOFs according to the optimized L_k profile obtained in the previous section. A commercial step-index single-mode fiber (Thorlabs, SM800) is fixed with two fiber clamps (Thorlabs, T711/M-250) on stepper-motor-driven

linear translation stages (SURUGA SEIKI, KX1250), which pull the fiber on both ends at a velocity of $v_1 = 15\ \mu m/s$. The fiber is heated with a flame from a hydrogen torch whose stainless-steel nozzle has a single hole with an inner diameter of 135μm. We use pure hydrogen gas (no premix with oxygen), and the gas flow is adjusted to 10mL/min by a flow meter (KOFLOC, RK1250). The torch is also mounted on a stepper-motor-driven stage and scans along the fiber with a velocity of $v_2 = 750\ \mu m/s$. Light from an 852 nm laser diode is coupled to a 99/1-fiber beam splitter, and the 99 % output port is fusion spliced to the fiber being pulled. We stabilize the laser output power to within $\pm 0.1\%$ by monitoring the power from the 1% port and feeding it back to the diode current. The TOF transmission is measured throughout the pull.

We fabricate TOF optimized for the adiabaticity factors of $F = 0.2$, 0.4, 0.6, and 0.8. For comparison, we also fabricate TOF with two other shapes. One TOF has a constant taper angle of 2 mrad for $r > 4\mu m$ and an exponential shape with a waist length of 400 μm for $r < 4\ \mu m$. Note that all of the optimized TOF also have an exponential shape with a waist length of 400 μm for $r \leqslant 4\ \mu m$ because we fix L_k as $L_k = 400\ \mu m$ for $r_k \leqslant 4\ \mu m$. The other TOF has an exponential shape with a waist length of 3 mm. Five samples are fabricated for each profile. All samples are tapered to a waist radius that is thin enough to be single-mode guided ($r \leqslant 300$ nm).

Fig. 4 shows the change of the transmission during the pull for a TOF with $F = 0.4$. The amplitude of the oscillation due to the coupling to higher-order modes is small, and the final transmission is in excess of 99.7%. The disappearance of the oscillation is clearly observed at the end of the pull, which is also confirmed with the short-time Fourier transform (spectrogram) of the transmission trace[25]. The disappearance of the oscillation indicates the single-mode guidance.

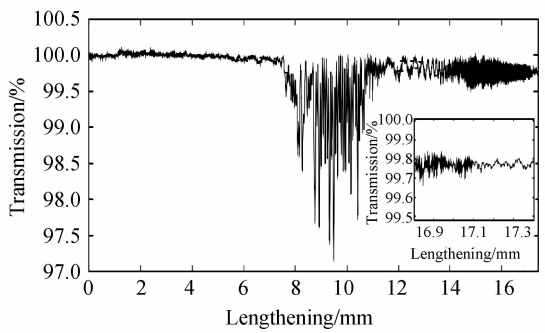

Fig. 4 TOF transmissio amplitude changes

Fig. 5 summarizes the transmissions of all the fabricated TOF. The transmissions of fabricated TOFs with the adiabaticity factors of $F = 0.2$, 0.4, 0.6, and 0.8, a constant taper angle of 2 mrad, and an exponential shape with a decay constant of 3mm. Five TOF are fabricated for each profile. The inset shows the transmissions for $F = 0.2$, 0.4, and 2 mrad with a magnified scale for the vertical axis. The relative error in the transmission is $\pm 0.1\%$, which is limited by the laser output power stability.

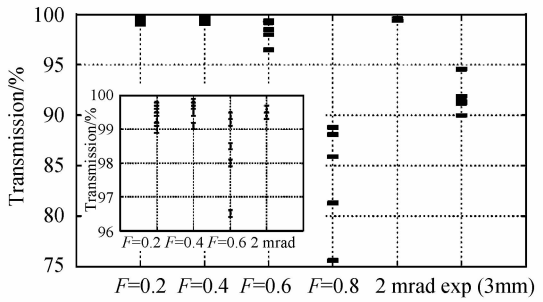

Fig. 5 TOF constant taper angle and transmission factors under adiabatic

There is a tendency that the profiles optimized with larger F values tend to have larger losses. Note that there are no noticeable differences in transmissions among the profiles of $F = 0.2$, $F = 0.4$, and the 2 mrad, in spite of the different taper angle profiles. This suggests that for these TOF the losses due to mode coupling are sufficiently suppressed, and other extrinsic losses are dominant. Indeed, Ravets et al. reported the transmissions of 99.95% for 2 mrad TOF[16-17]; the highest transmission measured in our experiment for 2 mrad TOF is only 99.6%. We suspect that the extrinsic losses for our TOF are primarily caused by contaminants on the TOF surface because we use a homemade clean hood of class 100000, compared to the class 100 clean room used in Refs. [16-17]. Furthermore, perturbations such as air, mechanical vibrations of the setup, and fluctuation of the gas flow may cause deviation of the TOF shape from the theoretical prediction, leading to less adiabaticity and larger losses.

We measure the shape of the fabricated TOF using a Scanning Electron Microscope (SEM). Fig. 6 shows the measured shapes for the $F = 0.4$ and 2 mrad TOF. In practice, the TOF have to be pulled over a longer distance than that predicted by the above model to achieve single-mode guidance at the waist. Longer pulling is required because of the effect of the finite flame width that is not negligible compared to the relatively small scan length L_{lower}. Thus, we extend the scan length profiles L_k to a larger scan number until single-mode guidance is reached, which is confirmed by the observed disappearance of the oscillation in the transmission (see Fig. 4). The predicted shapes in Fig. 6 are calculated with experimentally executed scan numbers. The TOF radii are measured as the half-width at the half-maximum of the each fiber edge slope

in the intensity profile of the SEM images, as shown in Fig. 7. The upper (lower) error bars are determined as the half-width at 10% (90%) of the maximum intensity of each slope. The SEM images at around the waist of TOF ($r \leqslant 4$ μm) are blurry due to the mechanical vibrations of the TOF, and the measured radii inevitably have large errors and may be overestimated (Fig. 7(a) and (c)), compared to those at $r \geqslant 4$ μm (Fig. 7(b) and 7(d)). However, because the delineation angle $\Omega(r)$ abruptly increases at $r \leqslant 4$ μm, precise knowledge of the TOF radius at these regions is not crucial to our study. For the regions with $r \geqslant 4\mu$m, the shapes of the fabricated TOF agree well with those predicted by the model with a normalized residual of $\leqslant 10\%$. Moreover, in spite of the higher transmission, the TOF with $F=0.4$ has almost three times shorter length (23 mm) than that for the 2 mrad TOF (63 mm). Note that the error bars around the waist of the TOF with $F=0.4$ are smaller than that for the 2 mrad TOF because TOF with $F=0.4$ has smaller mechanical vibrations due to its shorter TOF length.

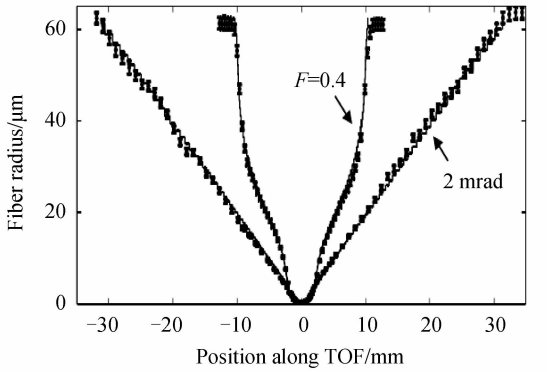

Fig. 6 TOF measurement shape of $F=0.4$ and 2 mrad

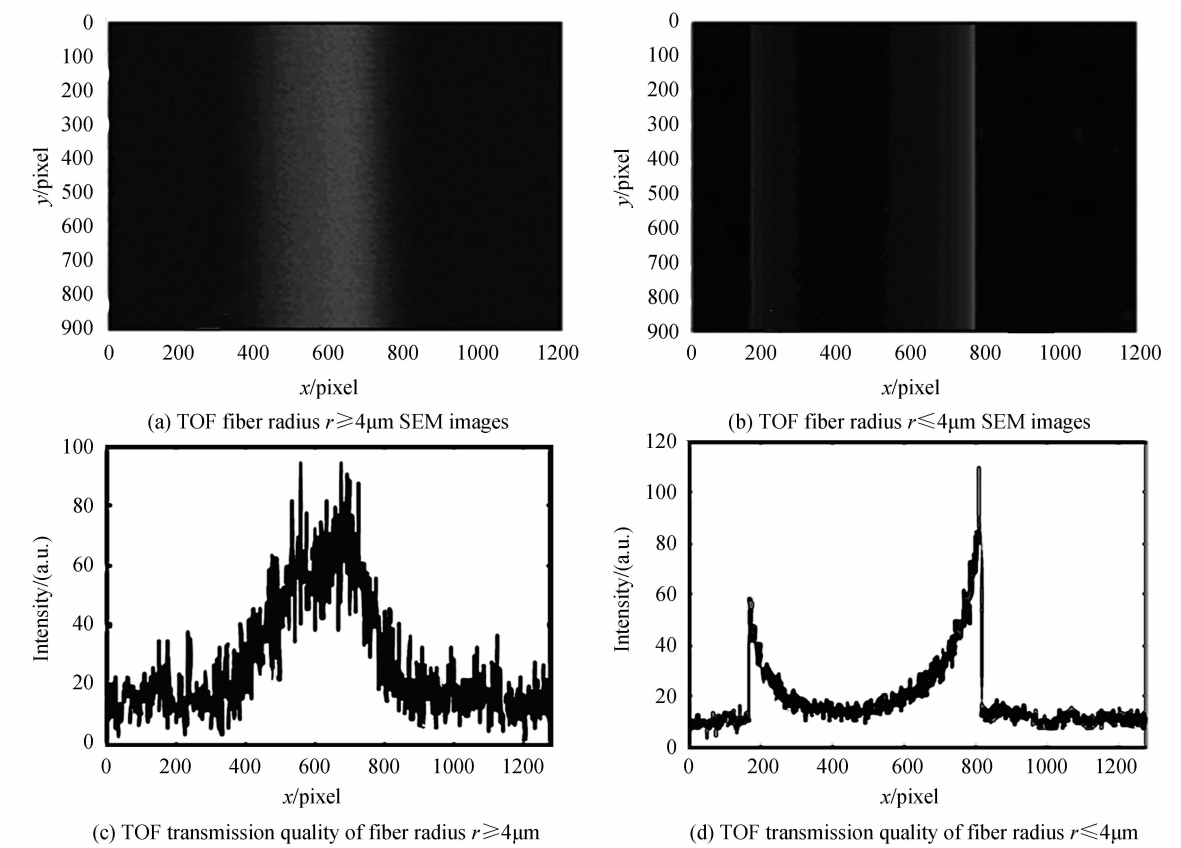

Fig. 7 Scanned images produced TOF shape

Fig. 8 shows the taper angles as a function of TOF radius for the fabricated $F=0.4$ TOF and 2 mrad TOF, along with the theoretically predicted taper angles for the optimized shape with $F=0.8$, 0.6, 0.4, 0.2, 2 mrad, and exponential TOF. The curves $F1$、$F2$、$F3$、$F4$, respectively TOF cone angle is a measure of the radius of 0.8、0.6、0.4、0.2; The curves M、E are 2 mrad and 3 mm exponential TOF; Circles and squares are $F=0.4$ and cone angle 2 mrad of TOF.

The measured taper angles of the $F=0.4$ TOF exceed the theoretical angles at around $30 \leqslant r \leqslant 40\mu$m. However, because the theoretical angles for the optimized profile coincidentally have much lower values than the targeted angles (0.4Ω) in this region, the measured angles do not considerably exceed the targeted angles. The highest transmission measured for TOFs with an optimal shape is in excess of 99.7 % with a total TOF length of only 23 mm, whereas TOFs with a constant taper angle of 2 mrad reach 99.6 % transmission for a 63 mm TOF length.

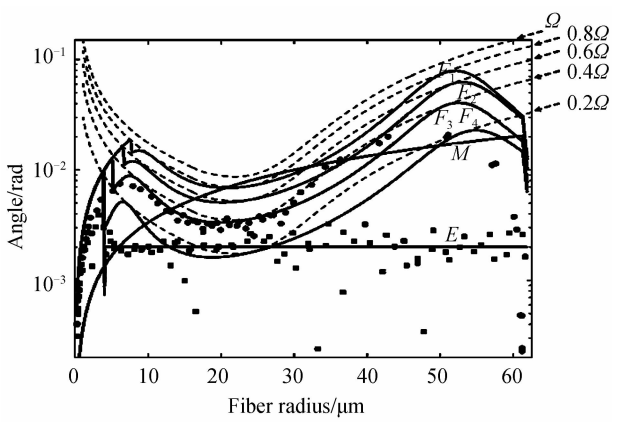

Fig. 8 Comparison of the predicted and measured taper angle

3 Conclusions

We have designed and fabricated TOF with high transmissions and minimal lengths. Transmission in excess of 99.7% has been observed for a TOF with a total length of 23mm. We find that the losses due to the power coupling to higher-order modes are sufficiently suppressed, and the losses are dominated by other extrinsic losses, such as contaminants on the TOF surface. Further improvement of the optimization may be possible by increasing the degrees of freedom for the approximation of L_k at the cost of longer computation time. This work will enable the production of compact, stable setups for coupling whispering-gallery-mode micro resonators to TOF without sacrificing the transmission quality. We plan to build such a setup for the study of cavity quantum electrodynamics with laser-cooled atoms and microtoroidal resonators.

References

[1] ALVARO F Z. Availability and cost analysis of PONs based on a network geometric model[J]. *Acta Photonica Sinica*, 2015, **44**(10):34-39.

[2] YANG Hai-ma, MA Cai-wen, WANG Jian-yu, *et al*. The transmission of polarized light of space atticude in quantum communication[J]. *Acta Photonica Sinica*, 2015, **44**(12):1227002.

[3] RAO Chun-fang, LIU Chen, YE Zhi-qing. Stress evolution sensing technique for electrodeposition based on fiber Bragg grating[J]. *Acta Photonica Sinica*, 2015, **44**(2):0206002.

[4] BRAMLE G. Optical fibre nanowires and microwares: A review[J]. *Optics Letters*, 2010, **22**(A 12):043001.

[5] DEASY K, FRAWLEY M. Manipulation and trapping of neutral atoms, molecules, and other particles using optical Nan fibers: A review[J]. *Sensors*, 2013, **42**(13):10449-10481.

[6] WADSWORTH W. Super continuum generation in tapered fibers[J]. *Optics Letters*, 2013, **25**(2):1415-1417.

[7] LEON S, BIRKS T. Super continuum generation in submicron fiber waveguides[J]. *Optics Letters*, 2014, **56**(12):2864-2869.

[8] GATES R, SASHA G. Super continuum generation in sub micrometer diameter silica fibers[J]. *Optics Letters*, 2015, **14**(3):9408-9414.

[9] ASIMOV D. Generation of a spectrally asymmetric third harmonic with unamplified 30-fs Cr: Forsterite laser pulses in a tapered fiber[J]. *Journal of Applied Physics*, 2013, **43**(B 76):515-519.

[10] GRUBSKY V. Glass micro-fibers for efficient third harmonic generation[J]. *Optics Letters*, 2015, **88**(13):6798-6806.

[11] LEE T, JUNG Y. Broadband third harmonic generation in tapered silica fibers[J]. *Optics Letters*, 2012, **36**(20):8503-8511.

[12] VIOLOR J. Fast detection of hydrogen with nano fiber tapers coated with ultra thin palladium layers[J]. *Optics Letters*, 2015, **56**(13):5087-5092..

[13] RUSSELL P. Photonic crystal fibers[J]. *Science*, 2013, **299**(12):358-362.

[14] BANG L. Selective detection of antibodies in microstructure polymer optical fibers[J]. *Optics Letters*, 2009, **109**(13):5883-5889.

[15] SURESH V. A fiber optic evanescent wave sensor used for the detection of trace nitrites in water[J]. *Optics Letters*, 2012, **24**(5):247-250.

[16] WYATT P. Fluorescent sensing using bucolical tapers Sense [J]. *Actuators*, 2013, **50**(B96):315-320.

[17] CURDIER E. Lateral access to the holes of photonic crystal fibers - selective filling and sensing applications[J]. *Optics Letters*, 2006, **109**(14):8403-8412.

[18] LEHH H, BRUCKNER S. Toward photonic crystal fiber based distributed chemo sensors [C]. 17th International Conference on Optical Fiber Sensors. SPIE, 2015: 419-422.

[19] WARKEN F. Ultra-sensitive surface absorption spectroscopy using sub-wavelength diameter optical fibers [J]. *Optics Letters*, 2007, **98**(15):11952-11958.

[20] GARCIA R. Ultra-sensitive fluorescence spectroscopy of isolated surface-adsorbed molecules using an optical Nan fiber [J]. *Optics Letters*, 2009, **99**(17):21704-21711.

[21] GARCIA R. Optical Nan fibers and spectroscopy [J]. *Journal of Applied Physics*, 2011, **102**(B105):3-15.

[22] KLIMOV V. Spontaneous emission rate of an excited atom placed near a Nan fiber[J]. *Physical Review*, 2014, **77**(A 69):013812.

[23] MORINAGA M. Optical Nan fiber as an efficient tool for manipulating and probing atomic fluorescence [J]. *Optics Letters*, 2007, **98**(15):5431-5438.

[24] SAGUE R. Optical interface created by laser-cooled atoms trapped in the evanescent field surrounding an optical Nan fiber[J]. *Physical Review*, 2010, **33**(104):203-206.

[25] KATO S. High-numerical-aperture microlensed tip on an air-clad optical fiber[J]. *Outlets*, 2014, **109**(39):773-778.